Gas Phase Precursor Chemistry in Carbon Nanotube Growth: a Reactive Molecular Dynamics and Quantum Chemistry Study

András Olasz[*1], *Péter Szelestey*[*1], *Tamás Veszprémi*[*2], *Gábor Varga*[*1,*2], *Tibor Höltzl*[*1]

ABSTRACT Gas phase chemistry of carbon nanotube (CNT) growth mechanism was investigated for different precursor molecules using state-of-the-art reactive molecular dynamics, which provides detailed insight into the time-dependent reactivity. Reactivity of different precursor molecules was examined and the chemical mechanisms of decomposition were determined. Quantum chemical computations enabled us to compute long-time chemical kinetics simulations based on the developed reaction mechanism in conjunction with rate coefficient computations. We concluded that the decomposition of hydrocarbon precursors takes place in two stages: the rapid formation of ethylene and acetylene followed by the slower conversion towards methane, which helps the understanding and serves the improvement of the CNT growth processes.

1. INTRODUCTION

Carbon nanotubes (CNT)[1] are one of the most promising materials in nanotechnology, due to their unique properties and structure. This can lead to several important applications, however, their application relies heavily on the development of efficient production methods[2]. The most favored synthesis method for their production today is catalytic chemical vapor deposition (CCVD) due to the good control, high purity and relatively modest reaction conditions[3]. In this process carbon precursors, catalyst and enhancers are injected into the high temperature reactor and the carbon nanotubes are grown on the catalyst nanoparticles. Efficiency of the process is determined not only by the conditions, but also on the applied catalyst and very importantly also on the carbon precursor[4), 5]. Therefore the development of efficient carbon precursors for CNT CCVD and understanding of their decomposition is very important[6), 7]. Besides hydrocarbons like methane, ethylene or acetylene as carbon precursors, more complex molecules, like cyclohexane[4], camphor[8], benzene[2], or substituted aromatic hydrocarbons[7] can be used efficiently. Successful application of ethanol showed that not only hydrocarbons, but compounds incorporating heteroatoms can also be used for carbon nanotube production[9].

While the CCVD process is performed in a tube reactor, the underlying chemistry is highly complex and the detailed understanding of the chemical reactions is still being investigated actively[10]. Particularly great attention is focused to explore the carbon nanotube growth mechanisms on the catalyst nanoparticles. Here atomistic modeling of the process plays a central role[10]. Molecular dynamics simulations enables detailed insights into the growth of single walled carbon nanotubes and the ring formation process. Catalytic role of the metal atoms and the effect of the substrate were investigated in detail[10), 11), 12), 13), 14), 15].

Growth of CNTs from more complex precursors was also investigated recently[16] and the importance of hydrogen atoms was emphasized[17]. Also, the role of the chemical potential of carbon in the precursor was found to play an important role[18), 19].

Carbon precursor decomposition starts before it is attached to the catalyst nanoparticle. Therefore the knowledge of the chemical reaction mechanisms and kinetics of the precursor decomposition is invaluable for the understanding and control of the CCVD reactor. Subsequently it is our aim to investigate the thermal stability of various aliphatic and aromatic precursors for CCVD synthesis of carbon nanotubes, determine their decomposition reaction mechanism and compute accurate chemical kinetics. For this reason we did rapid thermodynamic computations to determine the expected stability of the various precursors, then we determined the reaction mechanisms and compared the kinetics of the decomposition reactions using *high–temperature high–pressure* molecular dynamics. Finally, we used the reaction mechanism obtained in the previous step to compute accurate reaction rate coefficients and chemical kinetics.

2. METHODS OF COMPUTATIONS

Reactive molecular dynamics simulations were performed using the Large-scale Atomic/Molecular Massively

[*1] Furukawa Electric Institute of Technology
[*2] Budapest University of Technology and Economics

Parallel Simulator (LAMMPS) suite of programs[20] and the ReaxFF method[21] in conjunction with the force-field developed and tested for the combustion of hydrocarbons[22]. For the high-temperature high-pressure simulations 10 precursor and 200 hydrogen molecules were put into the simulation box, whose dimensions were chosen to provide internal pressure of 100 atm. Periodic boundary conditions were applied. The temperature was kept at 2000 K using a Nosé-Hoover thermostat with time constant of 100 fs. Integration time step was chosen to be 0.1 fs. 50,000,000 time steps were computed, which corresponds to a total simulation time of 5 ns.

The molecular dynamics trajectories were analyzed, molecules were identified and reactions were extracted using the ChemTraYzer software[23]. The Ovito program and Visual Molecular Dynamics program (VMD) with Tachyon were used for visualization[24), 25].

Based on the reaction mechanism obtained by high-temperature high-pressure molecular dynamics, quantum chemical computations were done using the Q-Chem 4.3 code. Equilibrium and transition state geometries were optimized and harmonic vibrational frequencies were computed using the ωB97X-D[26] functional in conjunction with the DEF2-SV(P) and the DEF2-TZVP basis sets[27), 28] as it is noted in the text. Subsequently, more accurate opposite spin-scaled double-hybrid XYGJ-OS[29] computations were carried out with the 6-311+G (3df, 2p) basis set, which has an accuracy of ~6 kJ/mol for thermochemistry and reaction barriers according to the test computations[29]. Thermochemical computations were performed using the Tamkin library[30]. Reaction rates were computed using the Transition State Theory for reactions with an energy barrier. Reaction rates of the association reaction were computed for barrierless reactions using collision theory, while the reaction rate of the dissociation reaction was computed using the principle of detailed balance.

Chemical kinetics simulations were performed using the Cantera library[31]. Unless otherwise noted, thermal and kinetics simulations were concluded at the more realistic temperature of 1500 K and at pressure of 1 atm, which can be computed conveniently and economically up to several seconds.

3. RESULTS AND DISCUSSIONS

3.1 Thermodynamic Modeling

Thermodynamic modeling provides valuable information about the driving force towards the decomposition of the precursors. As the pressure and the temperature are approximately constant in the growth zone of a CCVD reactor, we have computed the Gibbs-free energy of the precursor (C_nH_m) dissociation reaction towards ethylene (C_2H_4):

$$C_nH_m \rightarrow n/2\ C_2H_4 + (m/2 - 2n)\,H_2$$

Analogous reactions were considered for aromatic precursors, but with hydrogens at the reactant side. In order to compare the feasibility of the ethylene formation from various precursors, we define the relative reaction Gibbs-free energy by dividing the reaction Gibbs-free energy with the number of formed ethylene molecules.

Results in Figure 1 clearly show that aromatic precursors are noticeably more stable thermodynamically than the aliphatic precursors. It has to be noted that the relative reaction Gibbs-free energies change during the decomposition for benzene is nearly zero, while it is more negative in the case of toluene. This is attributed to the presence of the more active methyl group in the toluene. On one hand, the relative reaction Gibbs-free energy of the alkanes decrease with the size of the molecule, as the entropy increases greatly during the dissociation of the larger molecules. On the other hand, cyclohexane is more stable than any alkane, as it dissociates to three ethylene molecules and no hydrogen is formed. Along these lines the increase of entropy is smaller than in the case of aliphatic precursors.

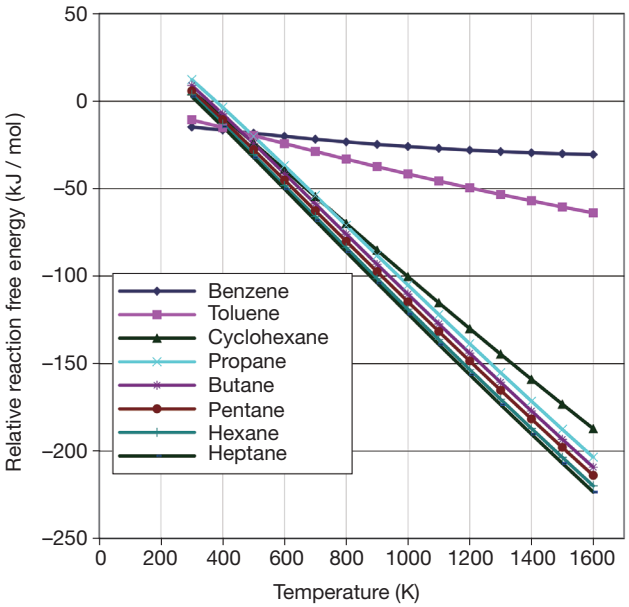

Figure 1 Relative free energy change during the decomposition of alkanes, one cycloalkane and aromatics to ethylene and hydrogen, computed using the ωB97X-D/DEF2-SV(P) method.

Our analysis shows that there is a striking thermal stability difference between aromatic and aliphatic compounds.

3.2 Reactive Molecular Dynamics Simulations

Reactive molecular dynamics simulations were shown to yield invaluable information in many highly complex chemical reactions[21] like combustion, catalysis, crystal growth, or polymers and successful application was also shown in the case of carbon nanotube growth simulations on catalyst nanoparticles[16), 17]. Here we apply this method for the simulation of the gas phase precursor decomposition reactions.

According to the above thermal analysis, aliphatic compounds are expected to dissociate towards ethylene if reaction time permits. This highlights the importance of the more detailed chemical kinetics simulations. It was shown recently that high-temperature high-pressure molecular dynamics is a valuable tool with a modest computational cost to determine the decomposition mechanisms of complex chemical compounds and also to get tendencies of the decomposition[23]. Reactive molecular dynamics shows the time dependence of the molecular system in a virtual reactor. A typical simulation setup is indicated in Figure 2. In this simulation the unit cell (under periodic boundary condition) is filled with hydrogen and the precursor. Chemical events take place as time progresses. Figure 2 also shows the dissociation of hexyl-radical to butyl radical and ethylene. Molecules are counted at every time step in order to identify individual reactions for the complete reaction mechanism.

Figure 3, 4 and 5 show the results of these simulations for various precursors.

It is well visible in Figure 3 that no chemical reaction was observed for benzene while dissociation of the methyl group of toluene was observed. In the case of toluene the simulation was continued for 15 ns without any change in the composition. Thus we can conclude that the dissociation of the methyl group is rather slow on the ns timescale.

The mechanism of the toluene decomposition is depicted in Figure 4. The reaction mechanism starts with the decomposition of one of the hydrogen molecules, which yields a hydrogen atom. This hydrogen is then attached to the carbon atom in ortho position compared to the methyl group of toluene. It is interesting to note that generally the combustion reactions also start with the formation of a hydrogen atom, which then leads to the set up of a radical reaction-chain. This similarity between the combustion reactions and the gas phase reactions in carbon nanotube CCVD is useful to interpret the resulting reaction mechanisms. During the next reaction step the additional hydrogen atom migrates to the methyl group and a methyl group is eliminated resulting in the formation of benzene. The methyl group then reacts with a hydrogen molecule, while a hydrogen radical forms. If the precursor concentration is large enough, this hydrogen radical can enhance the dissociation of further toluene molecules.

Overall, these simulations predict that aromatic rings

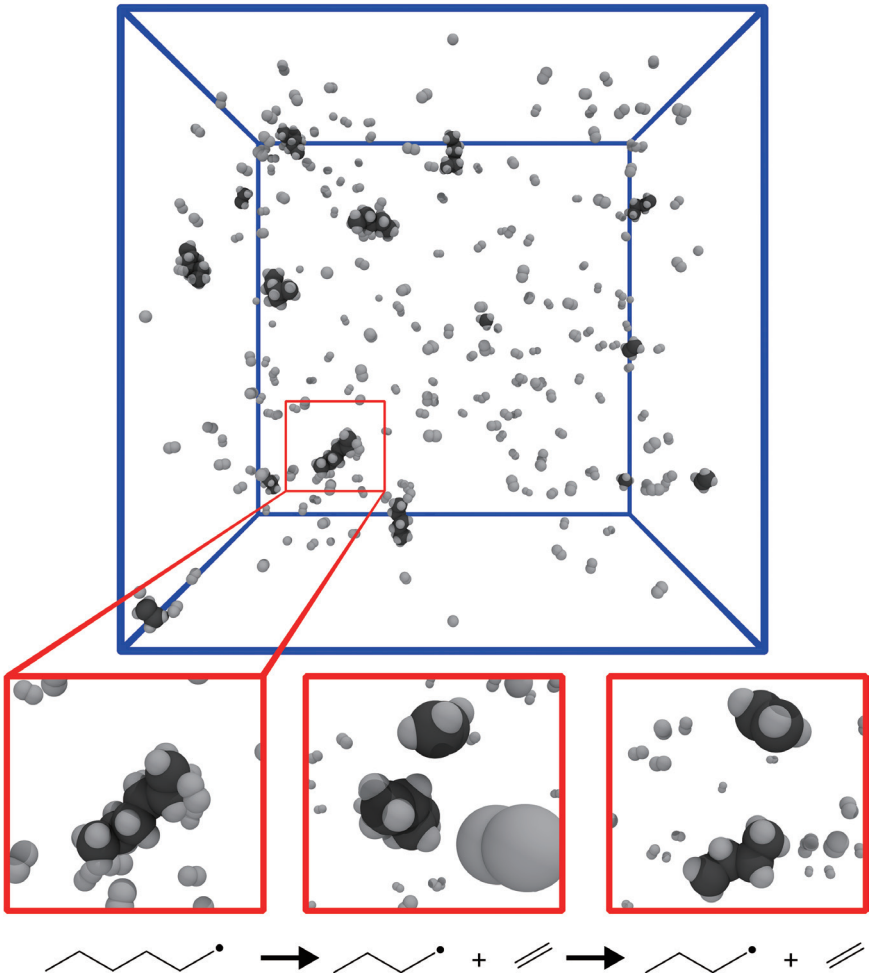

Figure 2 Virtual reactor: typical setup of a reactive molecular dynamics simulation. Carbon and hydrogen atoms are represented by grey and white spheres, respectively. Top figure shows the unit cell at a given time step, while bottom figures show a chemical reaction at subsequent time steps.

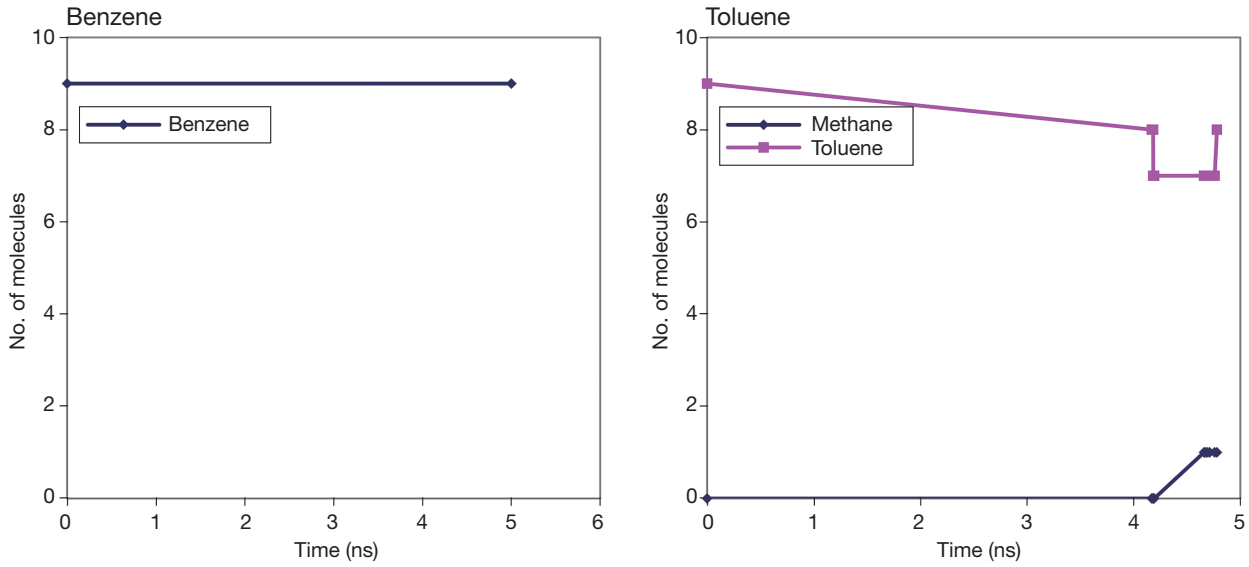

Figure 3 Decomposition kinetics of aromatic precursors using high-temperature high-pressure ReaxFF molecular dynamics.

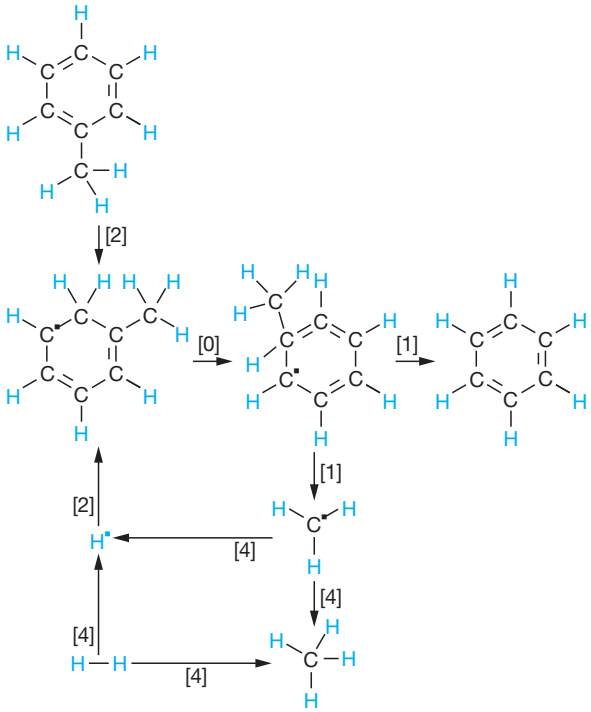

Figure 4 Decomposition mechanism of toluene.

are stable in CCVD and are expected to contribute directly to the carbon nanotube growth, which is in line with previous studies. Also, aliphatic side chains dissociate and induce further gas phase reactions.

As it is shown in Figure 5, the decomposition kinetics of aliphatic precursors is considerably more complex than that of the aromatic compounds and much diverse types of products form in these reactions. It is important to note that regardless of the aliphatic precursor compound the carbon chains gradually degrade by elimination of small hydrocarbons and the final products of the decomposition reactions are methane, ethylene and acetylene. Their formation rates and their ratio, however, depend sensitively on the precursor. Also, it is important that the intermediates of the chemical reaction mechanism depend considerably on the precursor. As theoretically any of the product or the intermediate of the dissociation reaction can participate in the carbon nanotube growth, these can lead to important differences in the efficiency of the different precursors.

As efficient dissociation of ethylene and ethylene radical (C_2H_3) from the precursor is important for efficient carbon nanotube growth[6], it is interesting to note that it forms from butane in a notable amount as a short-lived intermediate. On the other hand, in the case of hexane, propylene is an important intermediate, as it is an intermediate towards ethylene.

It is also visible in Figure 5 that the formation rate of ethylene increases with the length of the aliphatic chain, while an exceptionally large rate of ethylene formation is observed in the case of cyclohexane. These findings are in line with the expectations based on the thermal modeling.

Figure 6 shows the decomposition mechanism of hexane, obtained from molecular dynamics simulations. As the decomposition involves the shortening of the carbon chain by the gradual elimination of small organic compounds, this mechanism involves important reactions from the decomposition mechanism of smaller hydrocarbons, as well. This figure shows that the reactions start by the elimination of either a methyl group or hydrogen atoms, which then leads to the chain shortening. The resulting radicals re-arrange into branched chains, as branching is a well known stabilization mechanism of these compounds. Upon several similar elimination-rearranging steps we finally obtain methane, ethylene and acetylene as products.

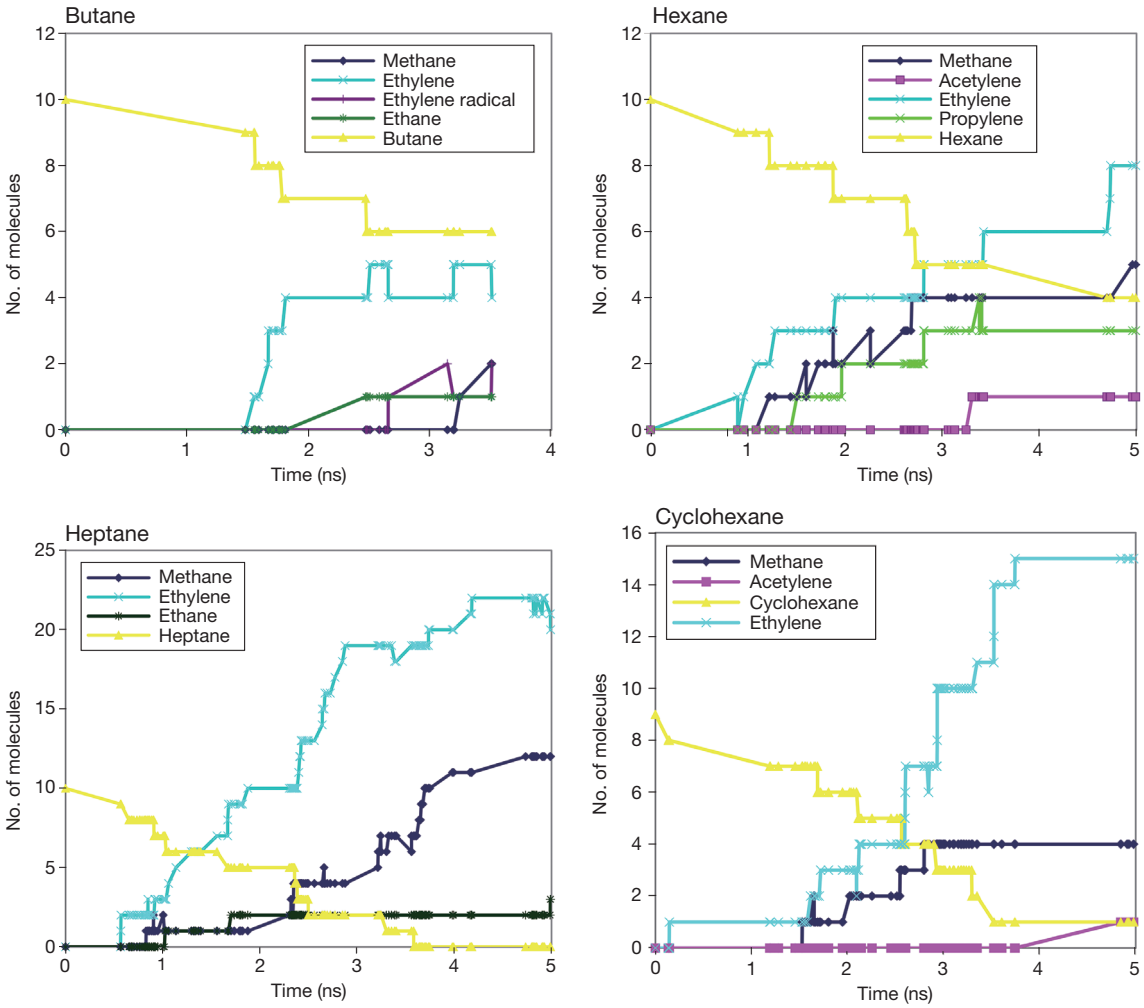

Figure 5 Decomposition kinetics of aliphatic precursors using high-temperature high-pressure ReaxFF molecular dynamics. The different precursors are marked by yellow lines.

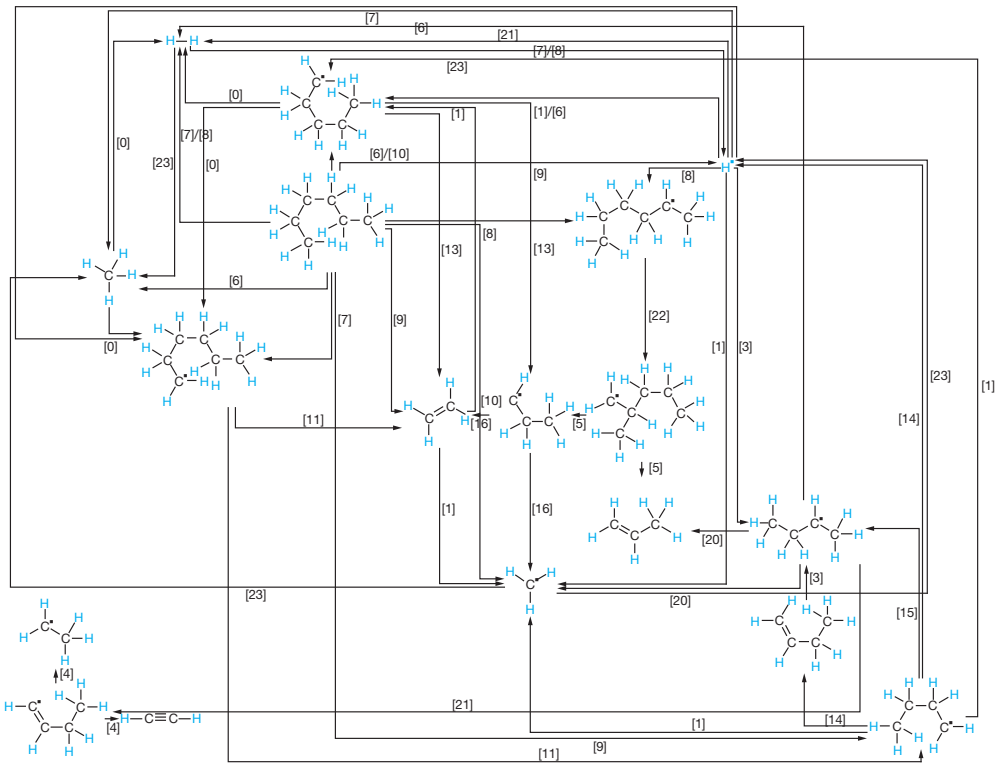

Figure 6 Decomposition reaction mechanism of hexane obtained from molecular dynamics simulations.

3.3 Quantum Chemical and Chemical Kinetics Simulations and Reaction Design

One of the most difficult part of the reaction rate simulations is the assembly of the reaction mechanism, as neglecting even a single important reaction may result in severe degradation of the applicability of the results. Therefore the reaction mechanism obtained using high-temperature high-pressure molecular dynamics simulations is invaluable to start the more accurate quantum chemical simulations. Temperature-dependent rate coefficients of all the reactions depicted in Figure 6 were recomputed as it is described in the methods section.

It is worth comparing the chemical kinetics simulations based on quantum chemistry to the results of the reactive molecular dynamics (Figure 7). Both simulations yield qualitatively similar picture: hexane decomposes rapidly to ethylene. Nevertheless, the simulations differ quantitatively, as the quantum chemical simulations are considerably more accurate than the reactive molecular simulations.

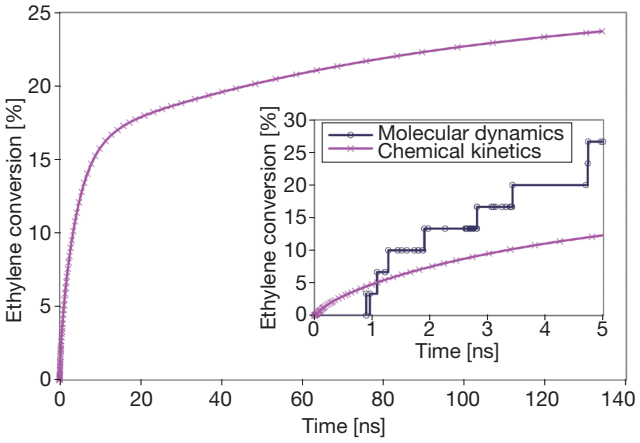

Figure 7 Hexane conversion to ethylene using reactive molecular dynamics and chemical kinetics simulations (based on quantum chemistry) at high-temperature high-pressure conditions (2000 K, 100 atm).

The developed reaction mechanism and the computed reaction rate coefficients make it easy to simulate the decomposition of hexane at arbitrary conditions, relevant for the carbon nanotube CCVD.

Figure 8 shows the result of simulations at 1200 K and 1 atm. The figure depicts that the onset of the hexane decomposition takes place at the microsecond time scale, much longer than at the high-temperature high-pressure conditions.

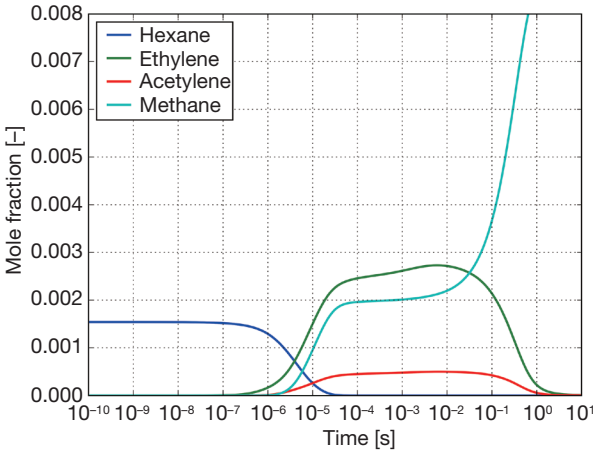

Figure 8 Hexane decomposition using chemical kinetics based on rate coefficients computed using quantum chemistry at 1200 K, 1 atm.

It can also be concluded from the figure that at long enough reaction times the final product of the decomposition is methane, the thermodynamically most stable compound at these conditions. The formation of methane takes place in two stages. First, at the microsecond time scale methane forms by the shortening of the carbon chain of the precursor, as we have seen earlier in the decomposition mechanism. Ethylene and acetylene form in this stage. Second, larger fraction of methane forms in the 0.1 second reaction time scale due to the further decomposition of ethylene and acetylene to methane. This has a profound consequence on the reactor optimization and design, as the activity of these compounds for the carbon nanotube growth are the following: acetylene>ethylene>methane. These can be fine-tuned using the residence time, temperature and also by the carrier gas because hydrogen has an important role in the decomposition.

4. CONCLUSIONS

Gas phase reactivity of hydrocarbon precursors in catalytic chemical vapor deposition process was investigated using reactive molecular dynamics and quantum chemistry based reaction kinetics methods. Reactive molecular dynamics was found to be useful to analyze the relative stability of the different precursors rapidly and also to set up reaction mechanisms, which serve as the basis of the more accurate quantum chemical computations.

The computations confirmed that benzene is highly stable at the typical synthesis conditions. Similarly toluene dissociates slowly into a methyl radical and benzene. In contrast to benzene, aliphatic precursors are highly reactive and dissociate rapidly. We found that dissociation takes place in two main stages. During the first stage mainly ethylene and acetylene and some methane forms in a few microseconds at 1200 K. As ethylene and acetylene are more active in the carbon nanotube growth than the parent compound, this is the activation stage of the

precursors. Details of the mechanism, chemical composition of the intermediates and the formation rate of ethylene all depend on the precursor composition. Cyclohexane dissociates more rapidly than the studied alkanes. In the case of alkanes the dissociation rate increases with the chain length. During the second stage ethylene and acetylene converts to methane, which is considerably less active than the previous compounds, thus this is the deactivation stage. Since the activity of the carbon source changes during the catalytic chemical vapor deposition process, the design target is to keep activity high by selecting appropriate thermal conditions, carrier gas and residence time.

Therefore these simulations contribute towards the simulation based improvement of the carbon nanotube CCVD process in the case of complex precursor molecules.

ACKNOWLEDGEMENT

The authors thank the Colleagues at FEC and FETI for the valuable discussions, suggestions and for their support.

REFERENCES

1) S. Iijima, Nature 354, 56 (1991).
2) E. Morinobu, T. Hayashi, Y. A. Kim, H. Muramatsu, Jpn. J. Appl. Phys. 45, 4883 (2006).
3) A. Oberlin, M. Endo, T. Koyama, J. Cryst. Growth. 32, 335 (1976).
4) M. Kumar, Y. Ando, J: Nanosci. Nanotechnol. 10, 3739 (2010).
5) K.A. Shah, B.A. Tali, Mat. Sci. in Semicond. Proc. 41, 67 (2016).
6) B. Shukla, T. Saito, M. Yumura, S. Iijima, Chem. Comm, 3422 (2009).
7) Y. Yamamoto, S. Inoue, Y. Matsumura, Diam&Rel. Mat. 75, 1 (2017).
8) M. Kumar, X. Zhao, Y. Ando, S. Iijima, M. Sharon, K. Hirahara, Mol. Cryst. And Liq. Cryst. 387, 117 (2002).
9) S. Maruyama, R. Kojima, Y. Miyauchi, S. Chiashi, M. Kohno, Chem. Phys. Lett. 360, 229 (2002).
10) V. Jourdain, C. Bichara, Carbon, 58, 2 (2013).
11) Y. Shibuta, S. Maruyama, Chem. Phys. Lett. 382, 381 (2003).
12) Y. Shibuta, Diam&Rel. Mat. 20, 334 (2011).
13) Y. Shibuta, S. Maruyama, Chem. Phys. Lett. 39, 842 (2007).
14) A. Page, Y. Ohta, S. Irle, K. Morokuma, Acc. Chem. Res. 43, 1375 (2010).
15) S. Irle, Y. Ohta, Y. Okamoto, A. J. Page, Y. Wang, K. Morokuma, Nano Res. 2, 755 (2009).
16) U. Khalilov, A. Bogaerts, E.C. Neyts, Nanoscale, 6, 9206 (2014).
17) U. Khalilov, A. Bogaerts, E.C. Neyts, Nat. Comm., 6, 10306 (2015).
18) Y. Magnin, A. Zappelli, H. Amara, F. Ducastelle, C. Bichara, Phys. Rev. Lett. 115, 205502 (2015).
19) M. He, H. Amara, H. Jiang, J. Hassinen, C. Bichara, R. H. A. Ras, J. Lehtonen, E. I. Kauppinen. A. Loiseau, Nanoscale, 7, 20284 (2015).
20) H. M. Aktulga, J. C. Fogarty, S. A. Pandit, A. Y. Grama, Patallel. Comput, 38, 245 (2012).
21) T. P Senftle, S. Hong, M. M. Islam, S. B Kylasa, Y. Zheng, Y. K. Shin, C. Junkermeier, R. Engel-Herbert, M. J. Janik, H. M. Aktulga, T. Verstraelen, A. Grama, A. C. T. van Duin, npj Computational Materials 2, Article number: 15011 (2016).
22) K. Chenoweth, A. C. T. van Duin, W. A. Goddard, III, J. Phys. Chem. A 112, 1040 (2008).
23) M. Döntgen, M.-D. Przybylski-Freund, L. C. Kröger, W A. Kopp, A.E. Ismail, K Leonhard, J. Chem. Theor. Comput. 11, 2517 (2015).
24) A. Stukowski, Mater. Sci. Eng. 18, 015012 (2010).
25) a) Humphrey, W., Dalke, A. and Schulten, K., J. Molec. Graphics 14, 33 (1996) b) J. Stone *An Efficient Library for Parallel Ray Tracing and Animation*, 1998, Computer Science Department, University of Missouri-Rolla c) http://www.ks.uiuc.edu/Research/vmd/
26) J.-D. Chai, M. Head-Gordon, Phys. Chem. Chem. Phys. 10, 6615 (2008).
27) F. Weigend, R. Ahlrichs, Phys. Chem Chem Phys.,7, 3297 (2005).
28) K.L. Schuchardt, B.T. Didier, T. Elsethagen, L. Sun, V. Gurumoorthi, J. Chase, J. Li, T.L. Windus, J. Chem. Inf. Model., 47, 1045 (2007).
29) I. Y. Zhang, X. Xin, Y. Jung, and W. A. Goddard III, Proc. Natl. Acad. Sci. USA 108, 19896 (2011).
30) A. Ghysels, T. Verstraelen, K. Hemelsoet, M. Waroquier, V. Van Speybroeck, J. Chem. Inf. Model. 50, 1736 (2010).
31) David G. Goodwin, Harry K. Moffat, and Raymond L. Speth. *Cantera: An object- oriented software toolkit for chemical kinetics, thermodynamics, and transport processes*. http://www.cantera.org, 2016. Version 2.2.1.